

Supporting Information

Benzeneselenol-Modified Gold Nanoclusters for Cancer Therapy

Le Wang ‡, Wenfu Zheng ‡, Xingyu Jiang *

MATERIALS AND METHODS

Materials. Benzeneselenol (Mw = 157.07) and tetrachloroauric acid ($\text{HAuCl}_4 \cdot 3\text{H}_2\text{O}$) were from Sigma (USA). Glutathione (GSH, Mw = 307.33) were from Alfa Aesar (USA). All other chemicals and solvents are reagent grade. Doxorubicin HCL (DOX) was from Dalian Meilun BioTech Co., Ltd.

Preparation and Characterization of Se₁Au₂ NCs. We prepared various Au NCs-capped with benzeneselenol through one-pot synthesis process with glutathione (GSH) as a reductant, avoiding complex ligand exchange processes. We added fresh GSH aqueous solution (100 mM, 0.6 mL) with different volumes of benzeneselenol (100 mM, 0.12 mL, Se₁Au₅ NCs (Se:GSH=1:5) and 0.3 mL Se₁Au₂ NCs (Se:GSH=1:2)). Then we mixed HAuCl_4 aqueous solution (20 mM, 2 mL) into the solution and kept the final mixture in 20 mL under mild stirring 500 rpm at 70 °C for 24 h. The selenol groups of benzeneselenol can concurrently bind to Au NCs via Au-Se bonds. We subsequently ultrafiltered the Se₁Au₂ NCs with a centrifuge (HeraeusMultifuge X1R, Thermo Fisher Scientific, USA) thrice with double-distilled water to remove the unreacted chemicals. The experimental parameters were as follows: 8000 rpm, 20 min at 4 °C. We synthesized Au NCs as the control group using the same method mentioned above without the addition of the benzeneselenol. We characterized the size and the Zeta potential of the Se₁Au₂ NCs using a transmission electron microscopy (TEM, Tecnai G2 F20 U-TWIN, FEI company, USA) and a Zetasizer Nano ZS (Malvern Company, England) respectively. We employed a X-ray photoelectron spectroscopy (XPS ESCALAB 250Xi, Thermo Fisher Scientific, USA) to detect the chemical element of Se₁Au₂ NCs after dropped samples onto a silicon slice and vacuum-dried overnight at room temperature. We measured the inductively coupled plasma analysis (ICP, iCAP 6300, Thermo Fisher Scientific, USA) to test the concentrations of Se₁Au₂ NCs.

We found that the more loading of Se the more uniform the structure, so we used Se₁Au₂ NCs for the following antitumor activity evaluation. In order to evaluate the stability, we analyzed the size changes of Se₁Au₂ NCs in different media (Dulbecco's Modified Eagle Media (DMEM) supplemented with 10 % FBS, Opti-MEM reduced serum medium, serum-free DMEM) at 37 °C for 24 or 48 h by dynamic light scattering (DLS).

Effects of Se₁Au₂ NCs on Tumor Cells. We evaluated the effects of Se₁Au₂ NCs on tumor cells (Panc-1, human pancreatic cancer cells), A375 (human melanoma cells), MCF-7 (human breast cancer cells), SW620 (human colorectal cancer cells) and B16 (mouse melanoma cells)) and non-tumor cells (HUVECs, human umbilical vein endothelial cells), and HAF (human aortic fibroblast cells) *in vitro* at different concentrations. We cultured the cells in DMEM containing 10 % fetal bovine serum (FBS, Invitrogen, USA) and 1 % penicillin-streptomycin (PS, MP Biomedicals, USA) at 37 °C with 5 % CO₂. All types of cells were incubated with different concentrations of the Se₁Au₂ NCs separately for 24 h. The original concentration of these cells is 10⁵ cells/mL and the cell viability was measured by a cell counting kit (CCK8, Dojindo, Japan). We measured the

absorbance at 450 nm by a microplate reader (Tecan infinite M200) and calculated using the following equation:

Cell viability (%) = $(OD_{\text{experiment}} - OD_{\text{blank}}) / (OD_{\text{control}} - OD_{\text{blank}}) \times 100\%$, where $OD_{\text{experiment}}$ is the absorbance of the cells treated with $\text{Se}_1\text{-Au}_2$ NCs (0 to 512 $\mu\text{g/mL}$), OD_{blank} is the absorbance of DMEM (negative control), and OD_{control} is the absorbance of cells without anything.

We cultured all different kinds of tumor cells (10^5 cells/mL) in culture plates (Costar, Corning, NY, USA) for 1d and then incubated with $\text{Se}_1\text{-Au}_2$ NCs (0 to 128 $\mu\text{g/mL}$) for 48 h. After rinse of the cells thrice with phosphate-buffered saline (PBS, Solarbio, pH 7.4), we stained the cells with Calcein AM/PI (Dojindo, Japan) and assessed the cell density and morphologies by laser confocal microscopy (LSCM, Zeiss LSM 710, Germany). All the experiments were performed in triplicate.

Western Blot, Cellular Uptake and Lysosomal Escape of $\text{Se}_1\text{-Au}_2$ NCs. We seeded 1 mL Panc-1 cells and HUVECs (10^6 cells/mL) and treated them with $\text{Se}_1\text{-Au}_2$ NCs, Se, and Au NCs respectively. After 12 h, we rinsed the cells 3 times with PBS and added appropriate volume of Radio Immunoprecipitation Assay (RIPA, Solarbio) with protease inhibitors for 5 min. Then we collected the assay products in a 1.5 mL tube and centrifuged them for 10 min (12000 rpm, 4 °C) to collect the supernatant, which was the total protein solution. We measured the protein content by a BCA kit (Applygen) according to the manufacturer's instruction. We subjected the protein to SDS-PAGE and electrotransferred the freshly prepared protein onto PVDF membranes under 200 mA for 1h. The membranes were blocked with blocking buffer containing TBST (1% Tween20, 5 % non-fat milk) 1 h at 4 °C. We added the primary antibodies overnight at 4 °C and incubated with an appropriate secondary antibody (Anti-LC3B antibody, ab48394) for 30 min at room temperature.

We cultured Panc-1 cells (10^5 cells/mL) and treated them with different concentrations (0, 2, 8, 32, 64, 128 $\mu\text{g/mL}$) of $\text{Se}_1\text{-Au}_2$ NCs respectively in a humidified incubator at 37 °C with 5% CO_2 . After rinsing the cells with PBS, we stained the cells with Rhodamine Phalloidin (Invitrogen, 5 $\mu\text{g mL}^{-1}$) and Hoechst 33342 (Sigma, 10 $\mu\text{g/mL}$) to visualize the location of $\text{Se}_1\text{-Au}_2$ NCs in the cytoskeleton and cell nuclei respectively.

We seeded 1 mL Panc-1 cells (10^5 cells/mL) in a confocal dish and treated them with $\text{Se}_1\text{-Au}_2$ NCs (128 $\mu\text{g/mL}$) for different time periods (1 h, 2 h, 4 h and 6 h) respectively to observe the cellular uptake. After rinsing cells with PBS, we stained the cells with Hoechst 33342 (Sigma, 10 $\mu\text{g/mL}$), fixed in 4 % paraformaldehyde (PFA, Leagene) solution for 10 min, and imaged with LSCM. We cultured the Panc-1 cells (10^5 cells/mL) for 24 h in the absence of serum, stained the cells with LysoTracker Blue (Invitrogen, 75 nM) for 2 h. After rinsing the cells with PBS, we incubated the cells with $\text{Se}_1\text{-Au}_2$ NCs (128 $\mu\text{g/mL}$) for different time periods (0 h, 0.5 h, 1 h and 2 h) to study the escape of nanocluster from lysosomes. At different time points, we observed the fixed cells by LSCM, setting excitation wavelengths of LysoTracker Blue DND-22 and $\text{Se}_1\text{-Au}_2$ NCs as 373 and 530 nm, respectively. All the experiments are performed in triplicate.

Toxicity Evaluation. The *in vitro* cytotoxicity of the $\text{Se}_1\text{-Au}_2$ NCs was evaluated by testing the viability of HUVEC cells. We assessed the cell density by counting cell number in three stochastically selected areas. We evaluated the biocompatibility of $\text{Se}_1\text{-Au}_2$ NCs by hemolysis assay. We centrifuged fresh rat erythrocytes at 1500 rpm for 15 min, and then rinsed the cells thrice with PBS. We diluted the 100 μL $\text{Se}_1\text{-Au}_2$ NCs and Au NCs in saline to different concentrations, mixed with 100 μL suspension of centrifuged erythrocytes and then incubated them for 3 h at 37 °C. We tested the optical density of the samples at 567 nm ($OD_{567\text{nm}}$) by a

microplate reader after centrifugation at 1500 rpm for 5 min. All the experiments were performed in triplicate.

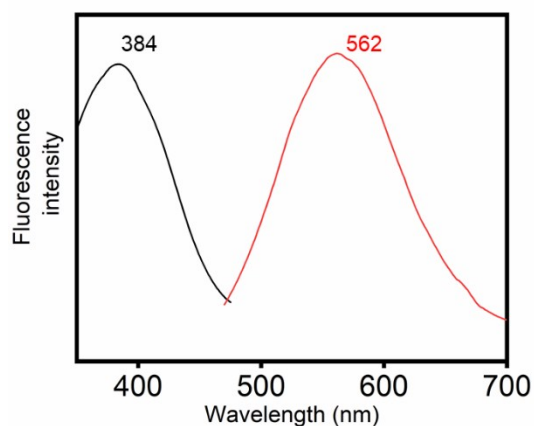
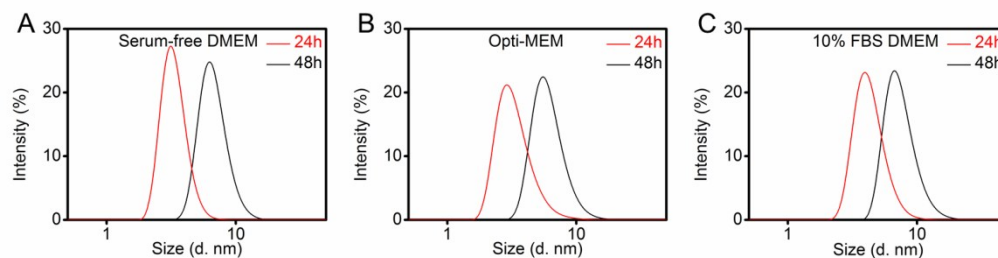
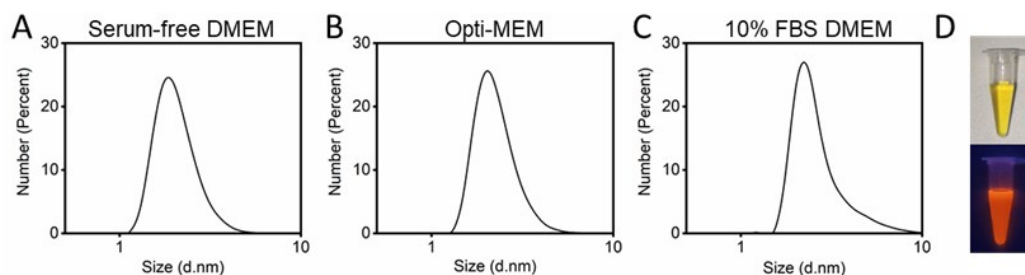
BALB/c mice (SPF grade, female, ~20 g, HFK Bioscience Co., Ltd, Beijing) were used to evaluate the toxicity. 15 mice were divided into three groups ($n = 3$) randomly. We injected different agents (Se₁-Au₂ NCs, 8 mg/kg; Se, 8 mg/kg; Au NCs, 8 mg/kg; and DOX, 8 mg/kg) into the mice every two days via tail vein respectively. After 14 days, we dissected tissues (heart, liver, spleen, lung, and kidney) for hematoxylin-eosin (HE) staining and observation by microscopy.

Animal Model. We developed two tumor models (subcutaneous tumor model, A375 cells) and orthotopic tumor model, Panc-1 cells) to evaluate the *in vivo* antitumor effect of Se₁-Au₂ NCs. For subcutaneous tumor model, we divided Balb/c nude mice (female, ~20 g) into 5 groups ($n=5$) and housed at a temperature of 24 °C and humidity of 55±10 %, with a 12 h light, 12 h dark cycle. We injected the A375 cells (100 μL, 10⁷/mL) subcutaneously near the mammary glands. The tumor volumes were determined by following equation: $V=0.5 \times w^2 \times l$, where V is the tumor volume (mm³), w is the width (mm), and l is the length (mm). When the final volume reached to around 5 mm in diameter, we injected different agents (Se₁-Au₂ NCs, 2 mg/kg; Se, 2 mg/kg; Au NCs, 2 mg/kg; and DOX, 1.94 mg/kg) into tumors every 2 days for 6 injections, setting PBS treated group as a control. For orthotopic tumor model, we divided the mice into 4 groups ($n=3$) and anaesthetized the mice with chloral hydrate (100 μL, 10 wt %). We injected Panc-1 cells (100 μL, 3 × 10⁷/mL) into the head of pancreas using a syringe. After two weeks of implantation, we injected the different materials (Se₁-Au₂ NCs, 4 mg/kg; Se, 4 mg/kg; Au NCs, 4 mg/kg; and DOX, 4 mg/kg) via tail vein every 2 days for 6 injections and monitored the weight and physiological conditions of the mice. After treatment, spleen and tumor were dissected for HE staining and observation by microscopy. Meanwhile, we collected and centrifuged the blood at 4000 rpm for 10 min and pipetted off the top yellow serum layer, and tested the levels of biomolecules in blood by ELISA kits (QuantiCyto) according to the manufacturer's instruction.

Statistical analysis. We used mean ± standard deviation (SD) to present data and analyzed the data with the student's *t*-test. The level of significance was defined at * $p < 0.05$, ** $p < 0.01$ and *** $p < 0.001$.

Table S1. Size distribution and Zeta potential of the Se₁Au NCs.

	Au NCs	Se ₁ -Au ₅ NCs	Se ₁ -Au ₂ NCs
Average size (nm)	2.46 ± 0.14	2.67 ± 0.10	2.50 ± 0.08
Zeta potential (mV)	2.10	-1.47	-6.61

**Fig. S1** Se₁Au₅ NCs emit intense orange fluorescence (562 nm) with the excitation at 384 nm.**Fig. S2** Variation of Se₁Au₂ NCs size in (A) serum-free DMEM, (B) Opti-MEM, and (C) 10% FBS-containing DMEM during different time periods.**Fig. S3** Characterization of Se₁Au₂ NCs after the storage at 4°C for 6 months in different media. Variation of Se₁Au₂ NCs size in (A) serum-free DMEM, (B) Opti-MEM, and (C) 10% FBS-containing DMEM is shown in the graphs. (D) Se₁Au₂ NCs solution shows clear yellow appearance under normal light conditions and emits orange fluorescence excited by UV light.

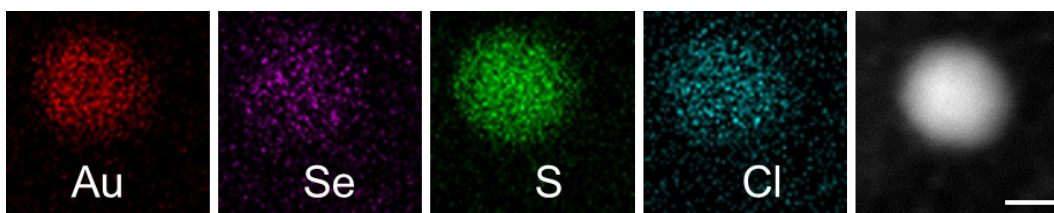


Fig. S4 Energy dispersive X-Ray mapping of Au, Se, S, and Cl elements in Se_1Au_2 NCs. Scale bars, 1 nm.

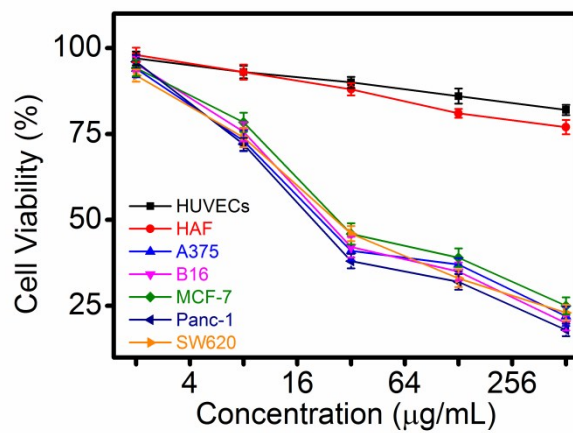


Fig. S5 Antiproliferative effect of Se_1Au_2 NCs against tumor cells and normal cells.

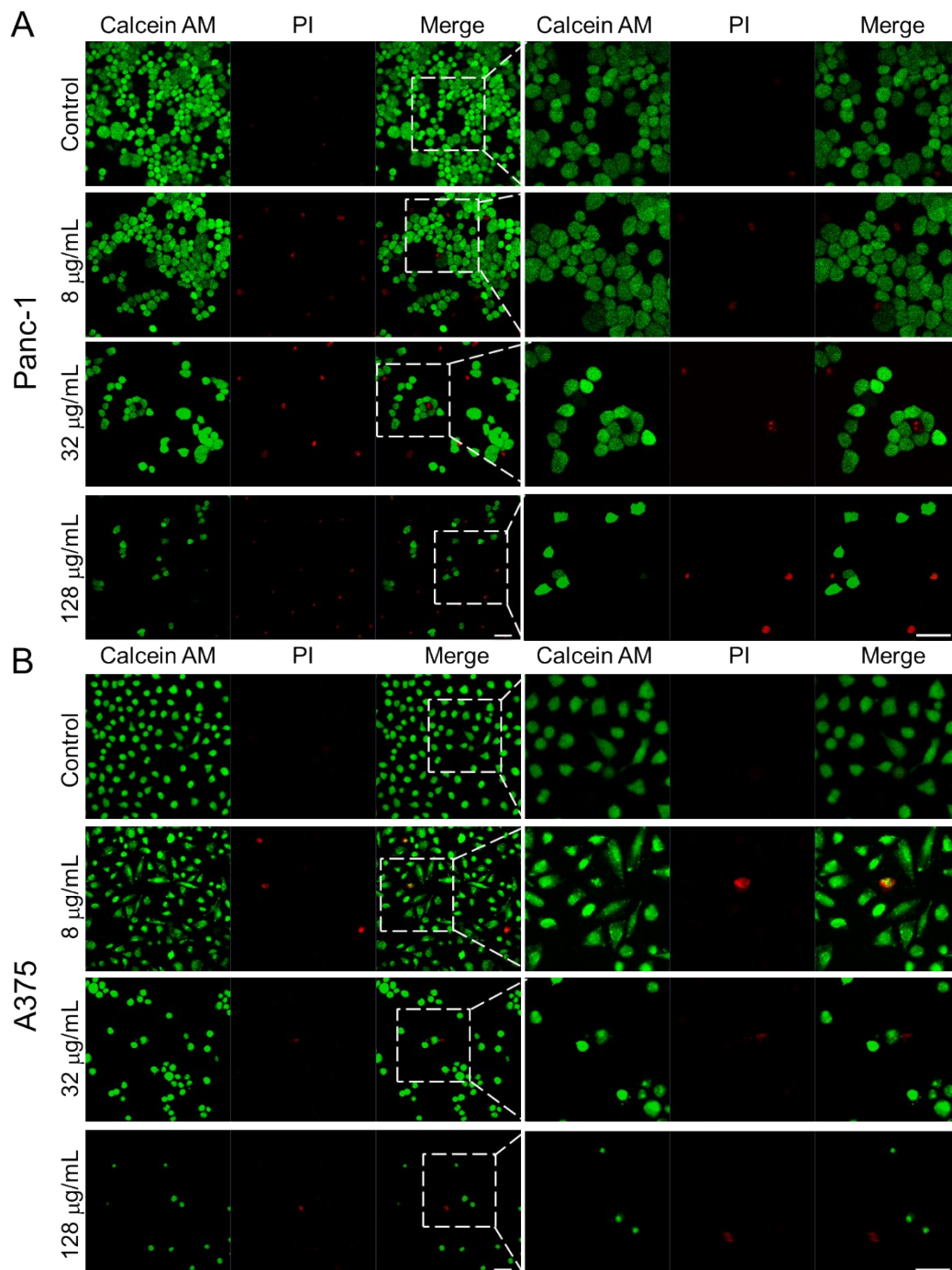


Fig. S6 The antiproliferative effect of $\text{Se}_1\text{-Au}_2$ NCs on tumor cells *in vitro*. (A) Confocal images of Panc-1 cells cultured with different concentrations of $\text{Se}_1\text{-Au}_2$ NCs. (B) Confocal images of A375 cells cultured with different concentrations of $\text{Se}_1\text{-Au}_2$ NCs. DMEM-treated tumor cells are used as a negative control. Scale bars, 50 μm . The images on the right panel are enlarged view of the left drawing areas.

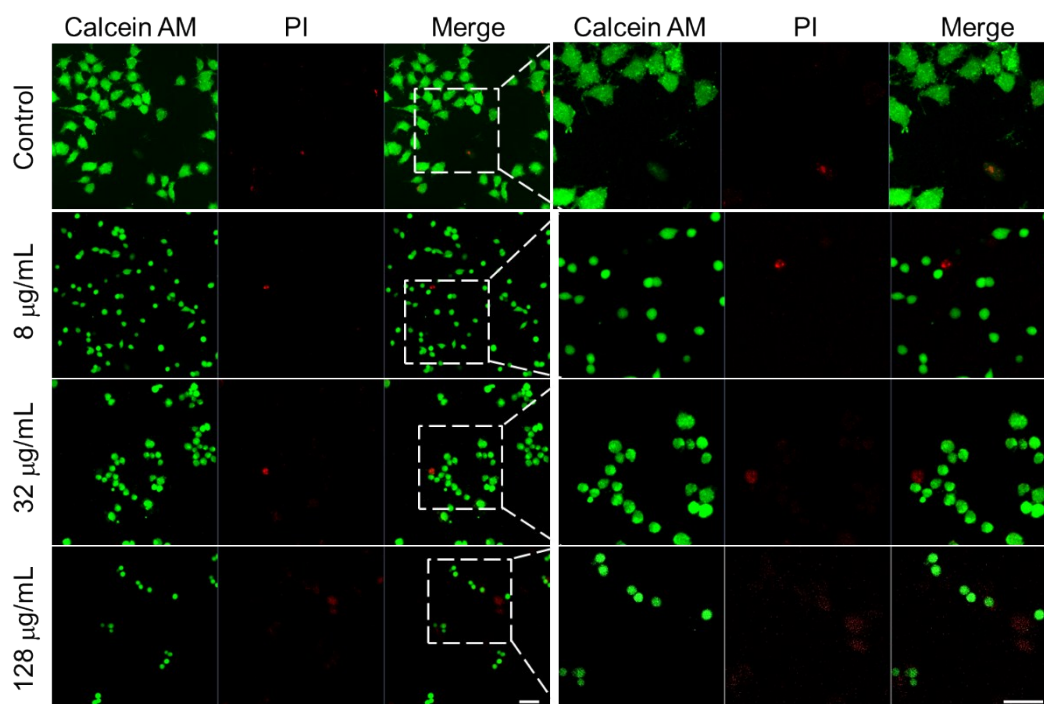


Fig. S7 Confocal images of MCF-7 cells incubated with Se_1Au_2 NCs of different concentrations. Scale bars, 50 μm . The images on the right panel are enlarged view of the left drawing areas.

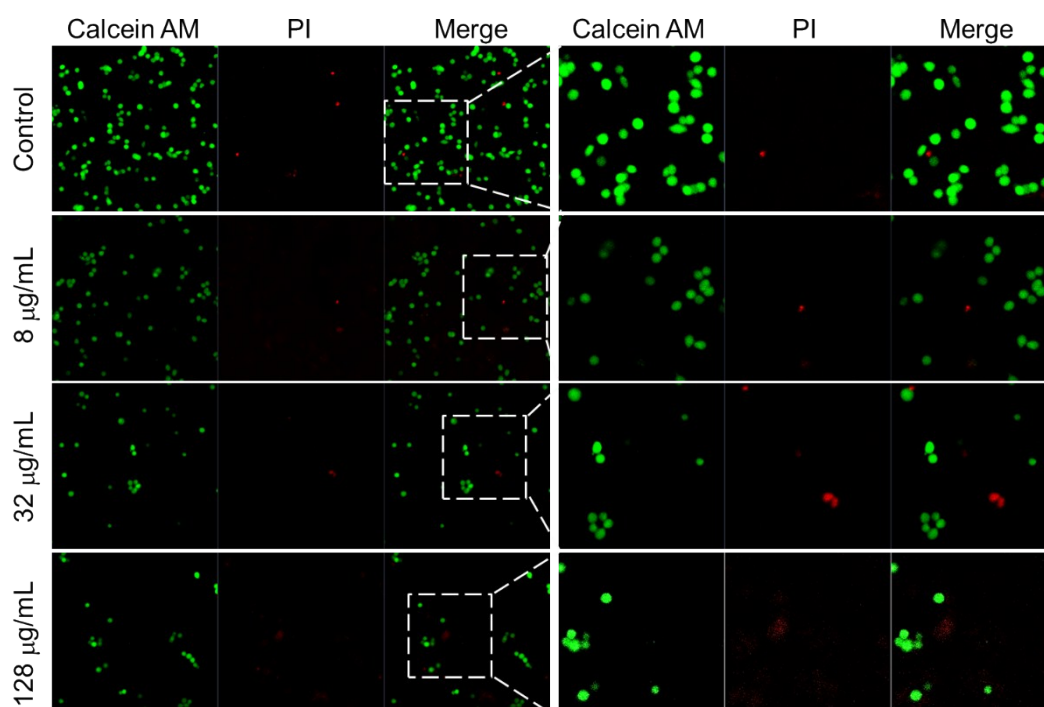


Fig. S8 Confocal images of SW620 cells incubated with Se_1Au_2 NCs of different concentrations. Scale bars, 50 μm . The images on the right panel are enlarged view of the left drawing areas.

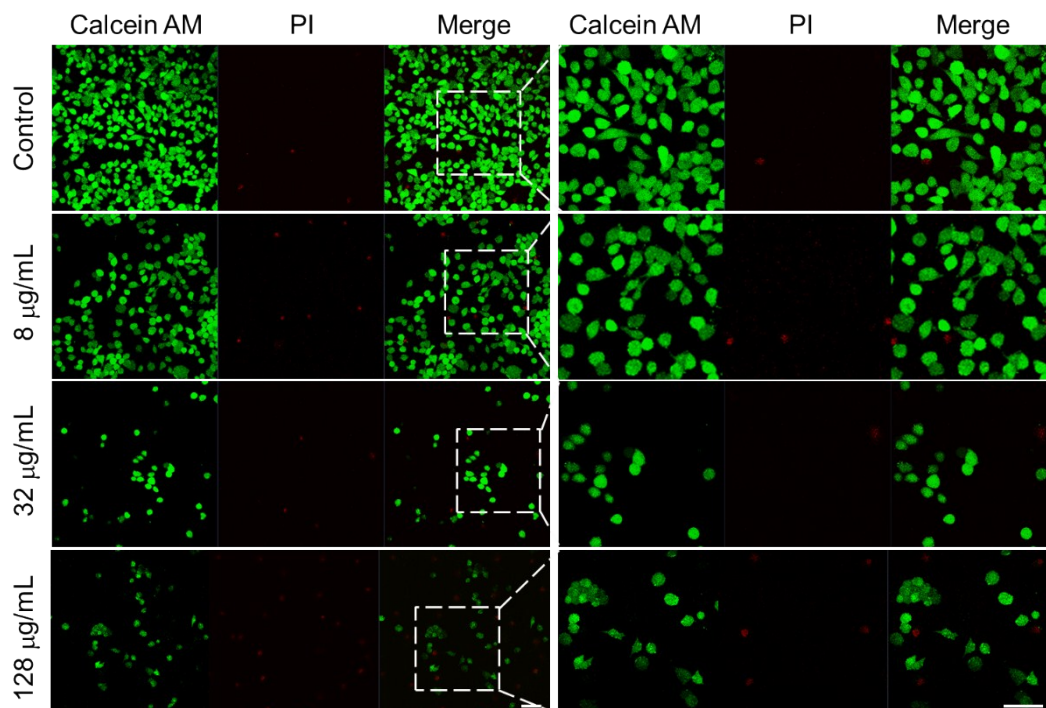


Fig. S9 Confocal images of B16 cells incubated with Se_1Au_2 NCs of different concentrations. DMEM is used as a negative control. Scale bars, 50 μm . The images on the right panel are enlarged view of the left drawing areas.

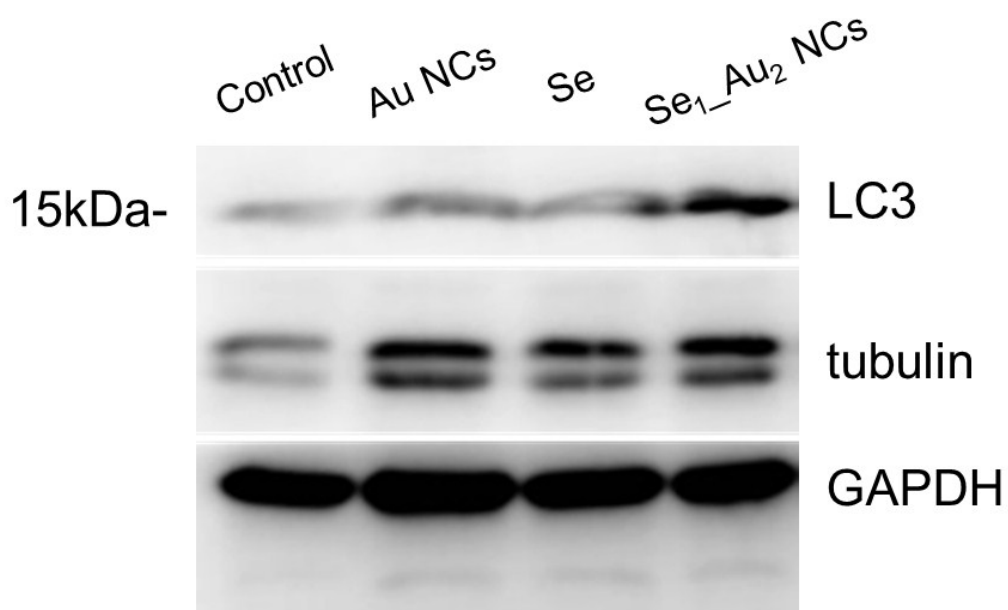


Fig. S10 Western blot of LC3 in Panc-1 cells treated by different agents.

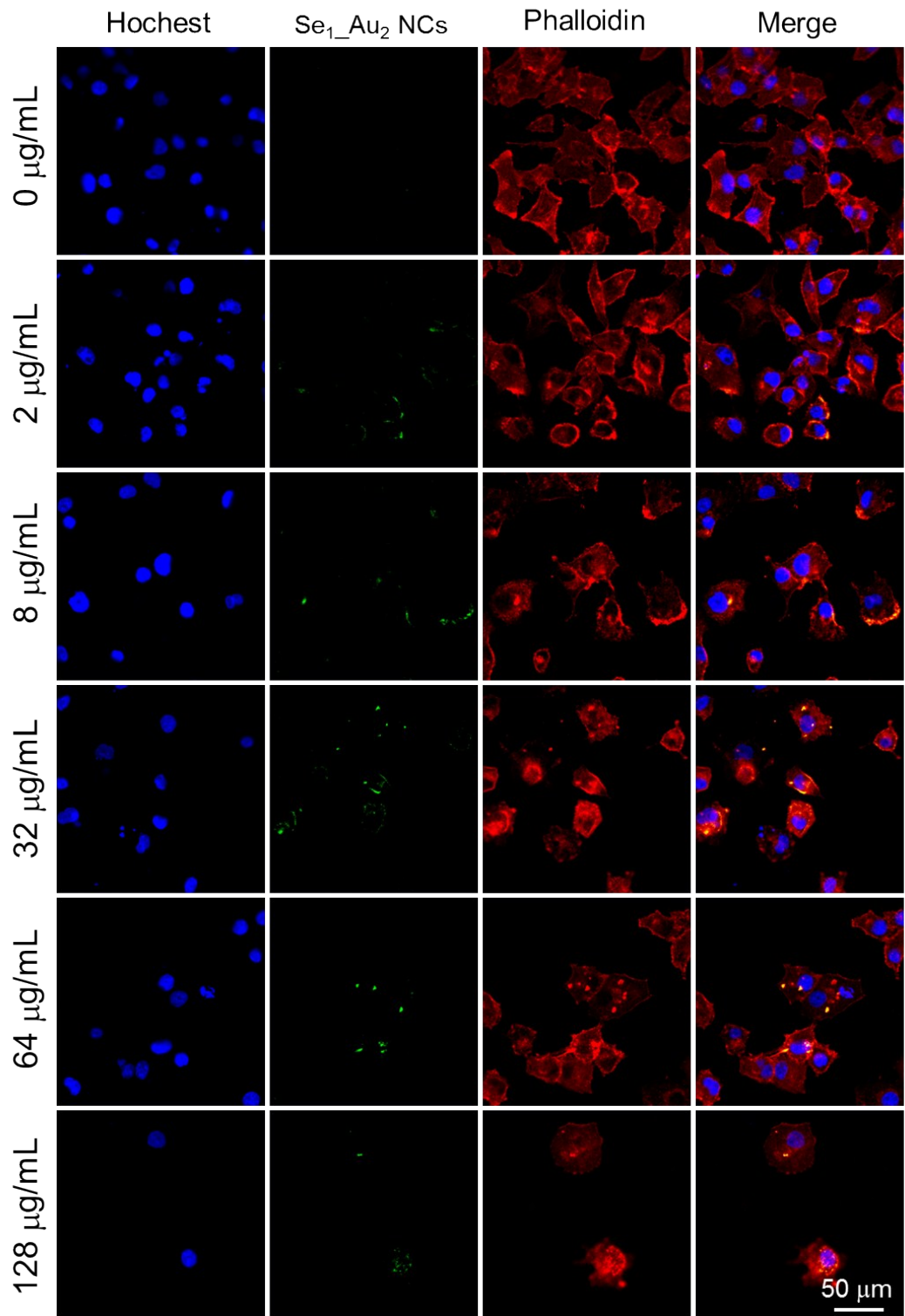


Fig. S11 Confocal images show Panc-1 cells treated by different concentrations of Se₁Au₂ NCs. Scale bars, 50 μm .

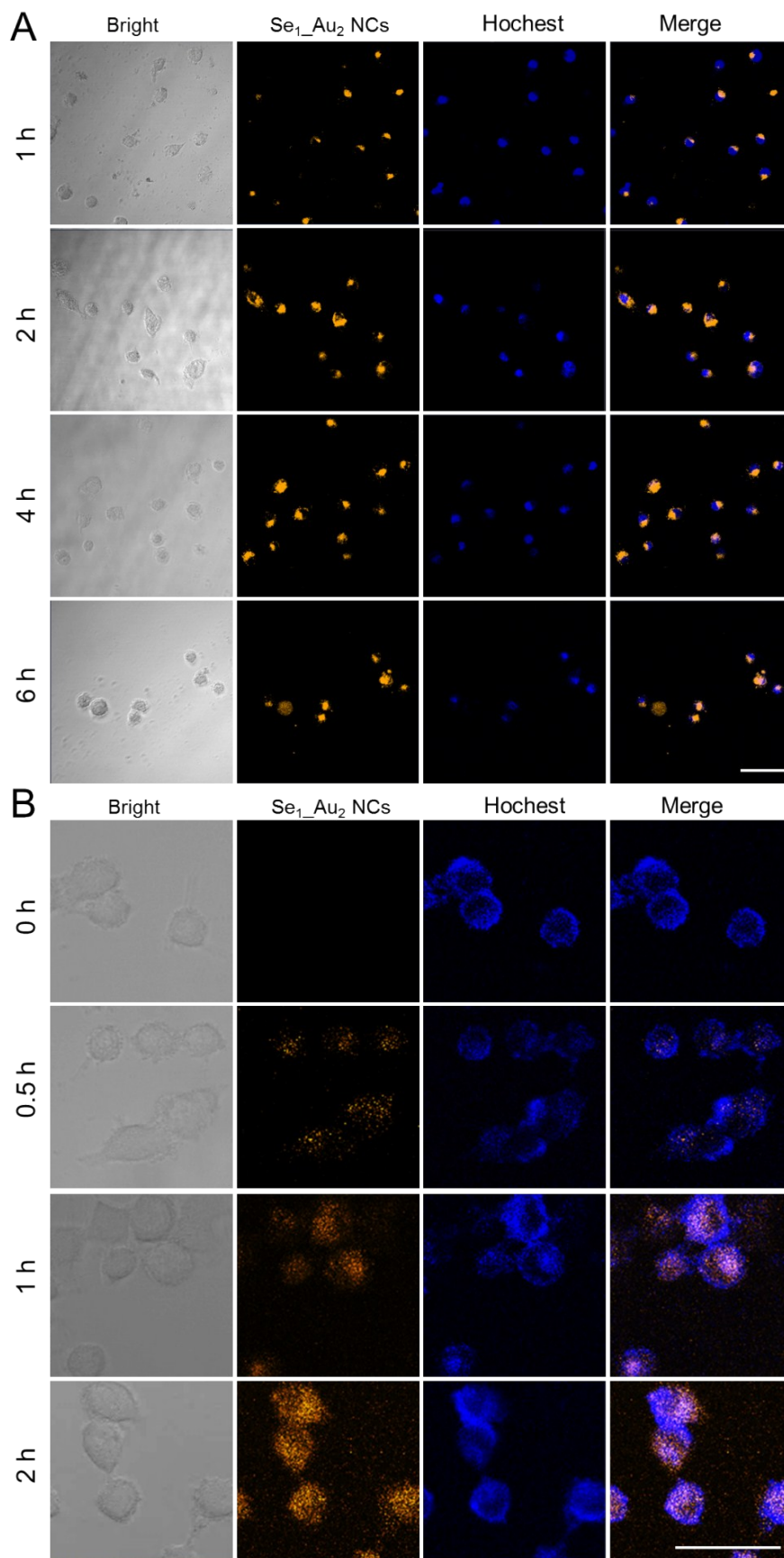


Fig. S12 Cellular internalization of Se₁Au₂ NCs formulations monitored by confocal

microscopy. (A) Cellular uptake of Se₁Au₂ NCs into Panc-1 cells at different time periods. (B) Lysosomal escape of Se₁Au₂ NCs in Panc-1 cells. Scale bars, 50 μm.

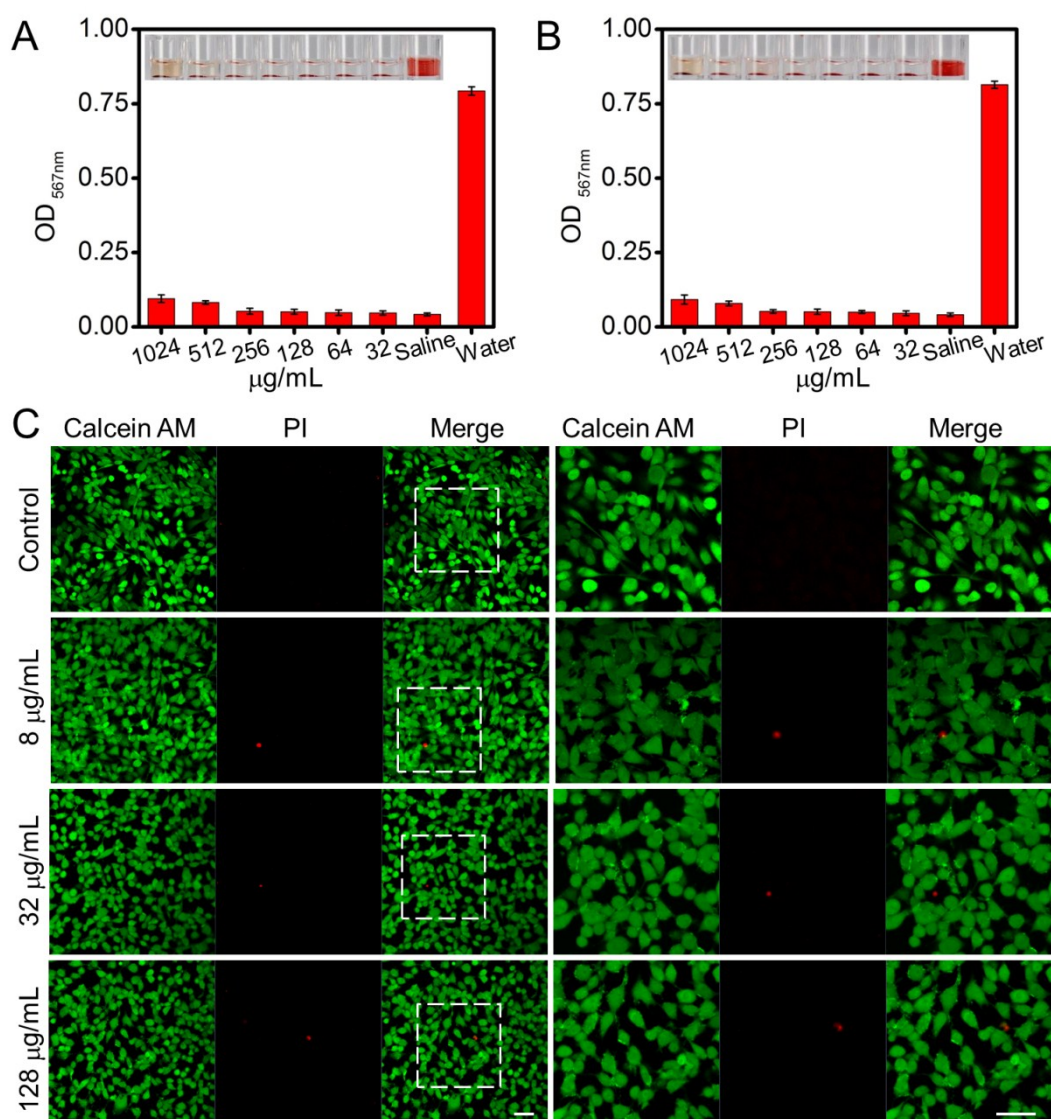


Fig. S13 Toxicity evaluation of Au NCs and Se₁Au₂ NCs. Fresh erythrocytes of SD rats are incubated with different concentrations of (A) Au NCs and (B) Se₁Au₂ NCs. Saline is used as a negative control and water is as a positive control. (C) Confocal images of HUVECs cultured with Se₁Au₂ NCs of different concentrations. Scale bars, 50 μm. The images on the right panel are enlarged view of the left drawing areas.

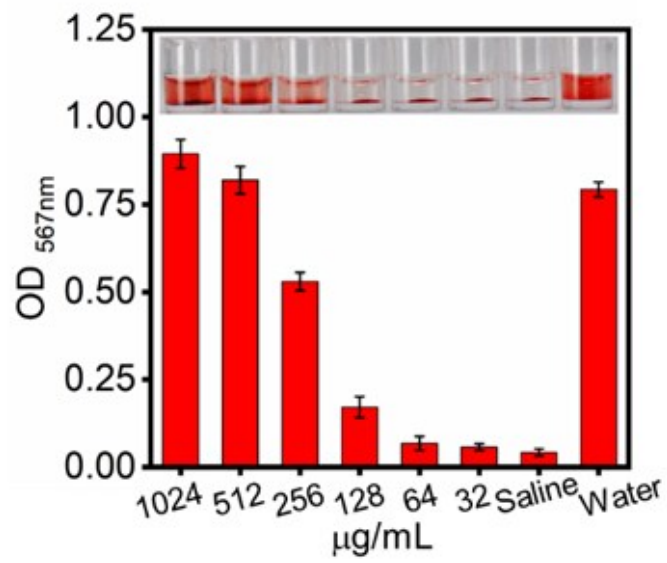


Fig. S14 Fresh erythrocytes of SD rats are incubated with different concentrations of benzeneselenol.

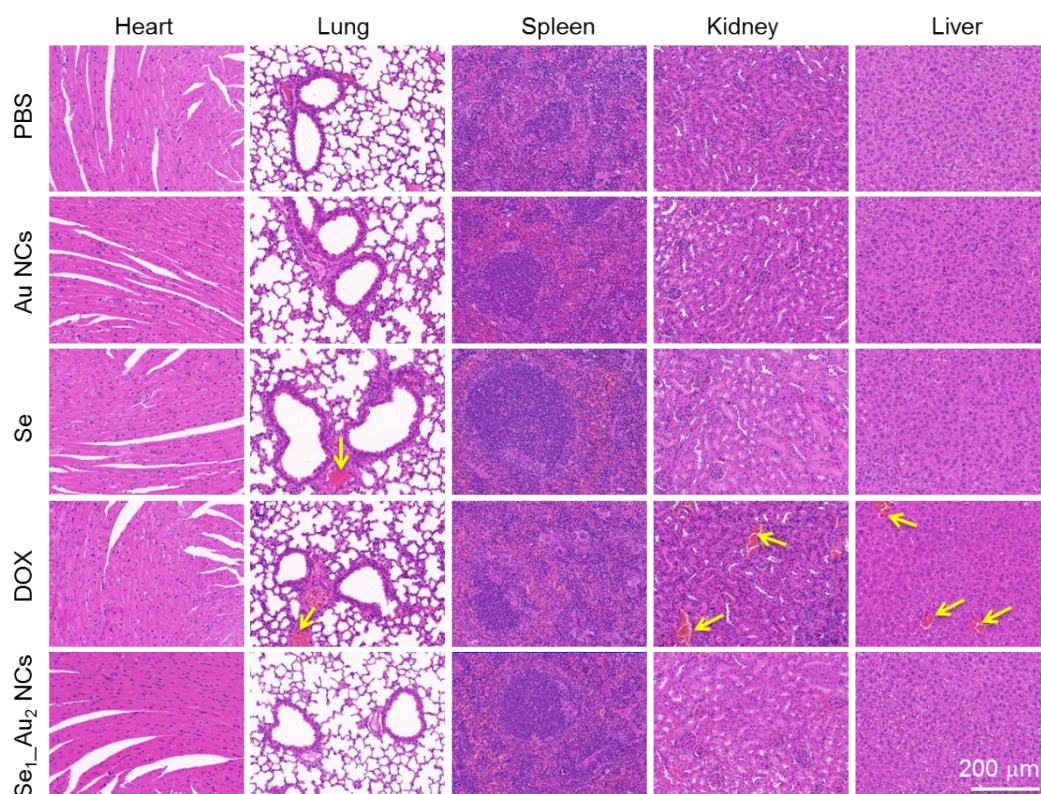


Fig. S15 HE staining of the excised tissues treated by different agents. Scale bars, 200 µm.

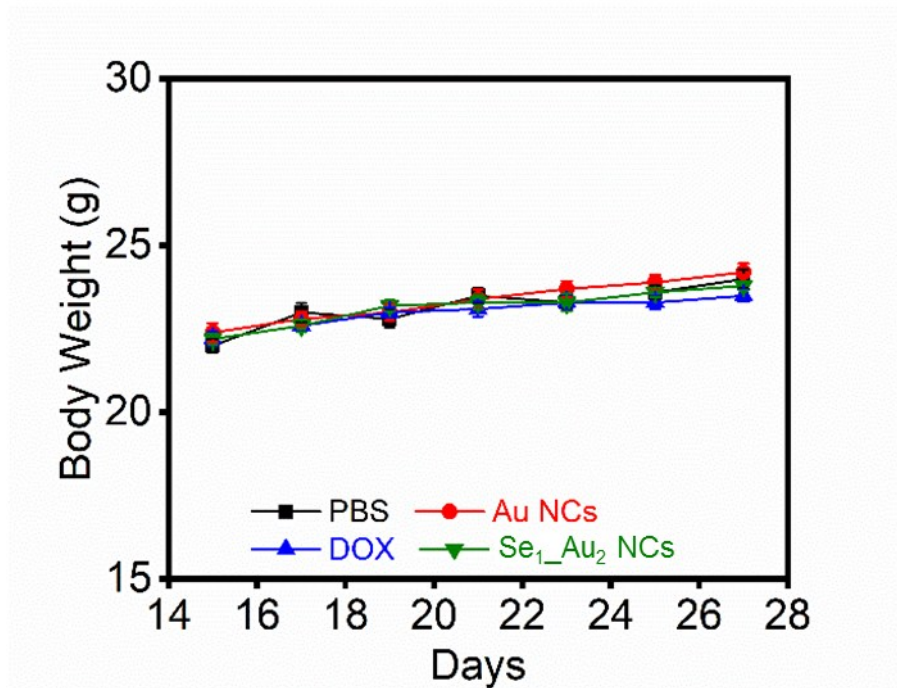


Fig. S16 The changes of the mouse body weight during treatments.

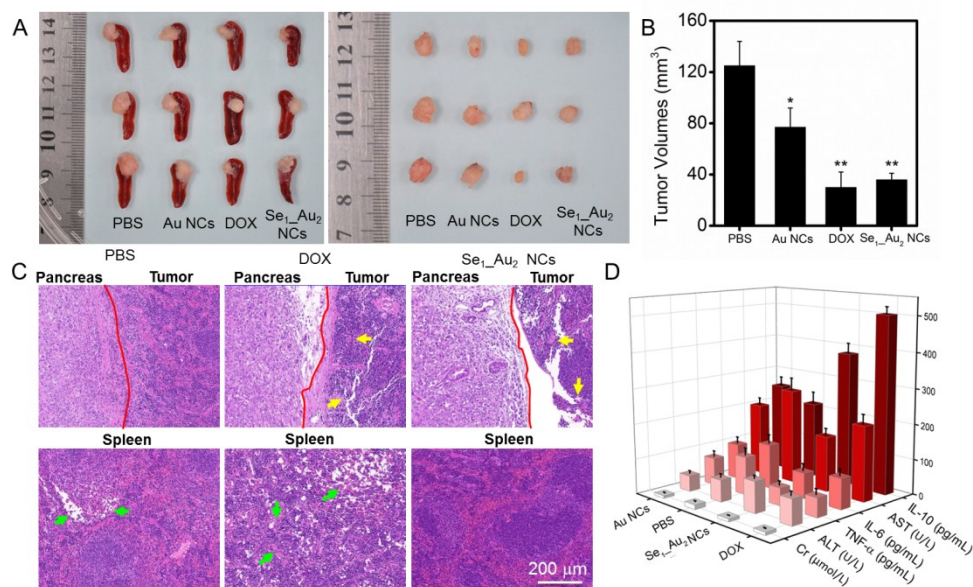


Fig. S17 The antitumor effects of Se₁Au₂ NCs in orthotopic pancreatic tumor model. (A) Macroscopic images of tumors under different treatments. (B) Tumor volumes after various treatments. (C) HE staining of the excised tumor tissue sections. (D) The level of different molecules indicating liver and kidney function, immunological and inflammatory response after different treatments.